Shaw and Shal voltage-gated potassium channels mediate circadian changes in *Drosophila* clock neuron excitability

Abbreviated title: Shaw and Shal mediate circadian excitability

Philip Smith[1], Edgar Buhl[1], Krasimira Tsaneva-Atanasova[2‡], and James J.L. Hodge[1‡]*

[1] School of Physiology, Pharmacology and Neuroscience, University of Bristol, University Walk, Bristol, BS8 1TD, UK

[2] Department of Mathematics and Living Systems Institute, University of Exeter, Stocker Road, Exeter, EX4 4QD, UK

[‡] The senior authors (K.Tsaneva-Atanasova@exeter.ac.uk (KTA); james.hodge@bristol.ac.uk (JJLH)) contributed equally to this work.

*Materials and corresponding author: Dr. James Hodge, ++44 (0) 117 331 1416, james.hodge@bristol.ac.uk

Abstract

Like in mammals, *Drosophila* circadian clock neurons display rhythms of activity with higher action potential firing rates and more positive resting membrane potentials during the day. This rhythmic excitability has been widely observed but, critically, its regulation remains unresolved. We have characterized and modeled the changes underlying these electrical activity rhythms in the lateral ventral clock neurons (LNvs). We show that currents mediated by the voltage-gated potassium channels Shaw (Kv3) and Shal (Kv4) oscillate in a circadian manner. Disruption of these channels, by expression of dominant negative (DN) subunits, leads to changes in circadian locomotor activity and shortens lifespan. LNv whole-cell recordings then show that changes in Shaw and Shal currents drive changes in action potential firing rate and that these rhythms are abolished when the circadian molecular clock is stopped. A whole-cell biophysical model using Hodgkin-Huxley equations can recapitulate these changes in electrical activity. Based on this model and by using dynamic clamp to manipulate clock neurons directly, we can rescue the pharmacological block of Shaw and Shal, restore the firing rhythm, and thus demonstrate the critical importance of Shaw and Shal. Together, these findings point to a key role for Shaw and Shal in controlling circadian firing of clock neurons and show that changes in clock neuron currents can account for this. Moreover, with dynamic clamp we can switch the LNvs between morning-like and evening-like states of electrical activity. We conclude that changes in Shaw and Shal underlie the daily oscillation in LNv firing rate.

Introduction

All organisms are subject to daily environmental changes caused by the earth's rotation; therefore, they have evolved circadian clock mechanisms that regulate changes in behaviour, physiology and metabolism to ensure their timely occurrence and thus allowing environmental adaption. The central circadian clock maintains a ~24-hour rhythm and in turn synchronizes the clock of peripheral tissues. Each clock neuron expresses core components of the molecular oscillator that switches itself on and then off roughly every 24-hours by a mechanism that is conserved from *Drosophila* to mammals including humans (Panda et al. 2002). Clock neurons show activity rhythms with higher spike firing rates and more depolarized membrane potentials during the day however the mechanisms driving this are not yet fully understood. Here, using a combination of electrophysiology, pharmacology, behaviour and computational modelling, we identify the voltage-gated potassium channels Shaw and Shal as underlying these rhythmic properties.

We studied this in the lateral ventral neurons (LNvs), a subset of the 150 *Drosophila* clock neurons that subdivides into large (l-) and small (s-)LNvs, broadly expressing the neuropeptide pigment-dispersing factor (PDF) barring the 5th s-LNv that is PDF-negative (Helfrich-Förster et al. 2007). PDF has an important role in morning anticipation and coordinating oscillations of the clock neurons with pdf^{01} null mutants being arrhythmic in constant darkness (DD) (Taghert and Shafer 2006). l-LNvs are known as wake-promoting arousal neurons (Parisky et al., 2008), while the s-LNvs are required to drive DD circadian rhythmicity (Helfrich-Förster et al. 1998); like other clock neurons they are also more depolarized and have a higher firing rate in the morning and these changes in membrane excitability are driven by the molecular clock (Sheeba et al. 2008; Cao and Nitabach 2008; Buhl et al. 2016).

Excitability of the LNvs is also important in regulating circadian locomotor behavioral rhythms. LNv hyperexcitation has been shown to disrupt nocturnal sleep (Sheeba et al. 2008). Conversely, electrical silencing of LNvs disrupts circadian rhythms (Wu et al. 2008) and imposing specific electrical activity patterns drives the transcriptional state of the neurons towards morning- or evening-like states (Mizrak et al., 2012). These rhythmic changes in membrane excitability are therefore important for sustaining the molecular clock, synchronizing molecular oscillations in different clock neuron groups and communicating circadian information from the clock to other regions of the brain and body that mediate circadian changes in physiology and behavior (Allada and Chung, 2010; Allen et al., 2017; Belle and Allen, 2018; Colwell, 2011; Flourakis et al., 2015; Kudo et al., 2011; Meijer and Michel, 2015; Mizrak et al., 2012; Nitabach et al., 2005).

Rhythmic changes in the membrane excitability of clock neurons are mediated by ion channels endogenously expressed in clock neurons (Itri et al., 2010; Meijer and Michel, 2015). Various channels have been implicated in the rhythmic changes in membrane excitability of clock neurons such as the sodium leak channel *narrow abdomen* which acts with a voltage-gated potassium channel (Flourakis et al. 2015) in the dorsal clock neurons (DN1) of *Drosophila.* In the LNv, the inward rectifier potassium channel, Kir, expression varies circadianly, peaking at dusk, in line with the hyperpolarization of the clock neurons at this time, Kir overexpression dampened the molecular clock and resulted in arrhythmic flies in constant conditions (Mizrak et al., 2012). While LNv expression of a tethered toxin to paralytic (voltage-gated sodium channel (Nav1)) has shown its importance in the phase of PDF release controlling rhythmic behavior (Wu et al., 2008). The photoreceptor, Cryptochrome when activated by blue light depolarizes l-LNv via a voltage-gated potassium

channel β-subunit, hyperkinetic assembling with pore forming subunits of voltage-gated potassium channels (Fogle et al., 2015). In the mammalian clock called the suprachiasmatic nucleus (SCN), the large-conductance calcium-sensitive potassium channel BK is important for the rhythmic changes in membrane excitability of clock neurons, protein levels vary circadianly and BK mutants change circadian behavior (Kent and Meredith, 2008; Meredith et al., 2006; Whitt et al., 2016), while the small-conductance calcium-sensitive potassium channel SK also controls rhythmic firing of clock neurons (Belle et al. 2009). Like in flies, Kir channels are also important for rhythmic changes in membrane excitability of clock neurons (Hablitz et al., 2014) and Nav1.1 is also expressed in SCN, with loss of function resulting in impaired SCN communication and circadian rhythms (Granados-Fuentes et al., 2012). Voltage-gated L-type calcium channels are also expressed in the SCN and control the rhythmic changes in membrane excitability of clock neurons (Diekman et al. 2013; McNally et al., 2019; Pennartz et al., 2002).

Transcriptomic studies of the LNvs have shown that mRNA levels of Shaker, Shab, Shaw, and Shal which are the *Drosophila* orthologues of the mammalian Kv1, Kv2, Kv3, and Kv4 respectively (Coetzee et al. 1999) vary circadianly with Shaw and Shal reported to vary transcriptionally (mRNA level of LNv clock neurons) with Shaw highest in the morning (ZT0) and Shal highest in the evening (ZT12) (Kula-Eversole et al. 2010). Kv3 and Kv4 mRNA, protein levels and currents were also both found to vary in the SCN, with mouse knock outs of the genes resulting in loss of rhythmic changes in membrane excitability of clock neurons and loss of behavioral rhythms (Itri et al. 2010; Itri et al. 2005; Kudo et al., 2011).

Shal/Kv4 is an A-type channel regulating neuronal firing (Gasque et al. 2005) including SCN firing rates and affects circadian rhythms with knock-down having

greater effect at night (Hermanstyne et al. 2017; Itri et al., 2010). Kv4.2 (Shal) and Kv1.4 (Shaker) are expressed in the SCN and loss of function mutants disrupt the clock neuron neuronal firing, circadian behavior and circadian period of PER2 expression, reiterating the importance and interdependence of the rhythmic changes in membrane excitability of clock neurons and the molecular clock (Granados-Fuentes et al., 2015; Granados-Fuentes et al., 2012; Hermanstyne et al., 2017). Additionally, block of Shal function by a dominant negative (DN) transgene in *Drosophila* has been associated with clock neuronal hyperexcitation, preferentially increasing clock neuron firing rates around ZT13 when rhythmic change in resting membrane potential and firing rate are low, disrupting PDF signaling to DN1 clock neurons (Feng et al. 2018). Shaw/Kv3 is critical for circadian modulation of SCN neuron activity, with the fast-delayed rectifier protein and current it mediates being higher during the day than at night. It remains higher during the day even during continuous darkness (DD) with blockade of Shaw/Kv3 preventing the rhythmic changes in membrane excitability of clock neurons (Itri et al., 2005). Kv3 knock outs greatly reduced fast delayed rectifier current resulting in a reduction in spontaneous activity in the day and reduced NMDA-evoked responses at night (Itri et al. 2005; Kudo et al. 2011). In *Drosophila* Shaw mediates a voltage-gated potassium current, with clock neuron expression of Shaw-DN and *RNAi*, increasing neuronal excitability and Shaw overexpression decreasing excitability. Expression of the transgenes in clock neurons remove the rhythmic changes in membrane excitability in terms of resting membrane potential and spontaneous firing rate which result in animals with changes in rhythmic PDF signaling, sleep, LD, DD and continuous light (LL) behavior (Hodge et al. 2005; Hodge and Stanewsky 2008; Parisky et al. 2008; Buhl et al., 2016).

Here we use whole-cell patch-clamping to investigate the electrophysiological properties of the LNvs and, using ion channel specific pharmacology, we show that Shaw and Shal display circadian rhythms in their activity. Behavioral analysis shows that they affect locomotor activity and lifespan. Finally, we build a computational model that, for the first time, allows the real-time manipulation of the LNvs using dynamic clamp and thus switching the LNvs between morning and evening states of neuronal activity.

Materials and methods

Fly husbandry

Flies were raised in a 12 h:12 h light dark (LD) cycle with lights on at ZT0 (Zeitgeber time) on standard *Drosophila* medium (0.7% agar, 1.0% soya flour, 8.0% polenta/maize, 1.8% yeast, 8.0% malt extract, 4.0% molasses, 0.8% propionic acid, 2.3% nipagen) at 25°C and collected between 0-5 days post eclosion. The following flies used in this study were previously described or obtained from the Bloomington or Vienna *Drosophila* stock centers: For wild type recordings, *RFP* fused to upstream regulatory elements of the *PDF* gene, *PDF-RFP* (Ruben et al. 2012), was used for identification of LNv neurons in all experiments. For channel manipulations, *PDF-Gal4* (Park and Hall 1998) was crossed to *UAS-Shaw-Truncated* (Bloomington *Drosophila* stock center (BDSC) stock 55748), a *Shaw dominant negative* (*Shaw DN*) transgene (Hodge et al. 2005) or *UAS-Shal pore 14* mutant the generates a *Shal dominant negative* (*Shal DN*) transgene (Ping et al. 2011). In order to block the molecular clock, *PDF-Gal4* was crossed to *UAS-CLKΔ5* (BDSC 36318) or *UAS-CYCΔ103* (BDSC 36317) canonical clock gene mutant transgenes (Tanoue et al. 2004). To validate the pharmacological blockers of Shaker and Shab, *PDF-Gal4* was crossed to *UAS-Shaker RNAi* (Vienna *Drosophila RNAi* stock KK104474) or *UAS-Shab RNAi* (BDSC 55682). For circadian rhythm experiments (Figure 4A-D) exclusively males were used, all other experiments used both males and females.

Electrophysiological recordings

Patch-clamp recordings were performed as described previously (Chen et al. 2015; Buhl et al. 2016). Briefly, brain explants of flies aged 0-5 days post-eclosion were dissected at several time-points: ZT1-3 (ZT2 i.e. 2 h after lights came on/early morning), ZT7-9 (ZT8), ZT13-15 (ZT14 i.e. 2 h after lights went off/early night), and ZT19-21 (ZT20). For recordings in darkness, dissections were conducted under red light illumination. Whole fly brains were dissected at room temperature (20-22°C) in standard extracellular solution containing (in mM): 101 NaCl, 1 $CaCl_2$, 4 $MgCl_2$, 3 KCl, 5 glucose, 1.25 NaH_2PO_4, 20.7 $NaHCO_3$, pH 7.2 on a M205C stereomicroscope (Leica, Wetzlar, Germany). The brain was positioned in the recording chamber and secured ventral side up using a custom-made brain harp. Neurons were visualized by RFP fluorescence using a 555 nm LED light source on an upright Zeiss microscope (Examiner.Z1, Carl Zeiss Microscopy GmbH, Jena, Germany). LNv neurons were identified on the basis of their fluorescence, position and size as the l-LNvs have a cell soma diameter of approximately 10-11 μm and the s-LNvs have a diameter of approximately 7 μm (Schubert et al. 2018). Whole-cell recordings were performed using glass electrodes with 8-18 MΩ resistance filled with intracellular solution (in mM: 102 K-gluconate, 17 NaCl, 0.94 EGTA, 8.5 HEPES, 0.085 $CaCl_2$, 1.7 $MgCl_2$ or 4 Mg·ATP and 0.5 Na·GTP, pH 7.2) and an Axon MultiClamp 700B amplifier, digitized with an Axon DigiData 1440A (sampling rate: 20 kHz; filter: Bessel 10 kHz) and recorded using pClamp 10 (Molecular Devices, Sunnyvale, CA, USA). A cell was included in the analysis if the access resistance was less than 50 MΩ as in other studies (Chen et al. 2015; Buhl et al. 2016) and was compensated by 70% on average.

Dynamic clamp recordings were performed using the CED Power 1401 system (Cambridge Electronic Design) and recorded using Signal (Version 6.05, Cambridge Electronic Design) at a sampling frequency of 10 kHz. The equations and parameters used are as shown in the 'Computational Modeling' section. Maximal conductance of channel models was adjusted as per Tables 2 and 3.

Circadian locomotor behavior

Analysis of locomotor activity of male flies was performed using the *Drosophila* Activity Monitor System (DAM2, Trikinetics Inc., Waltham, MA, USA) with individual flies in recording tubes containing standard food. The DAM monitors, were located inside a light- and temperature-controlled incubator (Percival Scientific Inc., Perry, IA, USA) where the fly's activity was monitored for 5 days in 12 h:12 h LD followed by 10 days in constant darkness (DD) at 25°C. Plotting of behavioral activity and period calculations were performed using a signal-processing tool-box (Levine et al. 2002) implemented in Matlab (MathWorks, Natick, MA, USA). All activity counts were recorded in 1-minute bins. Measurements of rhythmicity were performed by autocorrelation analysis (Levine et al. 2002); in short, each data-point is compared to other data-points at differing time intervals. The process is repeated for a range of intervals and this forms an autocorrelogram, in which the third peak gives a rhythmicity index from which the rhythmicity statistic (RS) is calculated.

Computational modeling

Computational modeling of ion channels and whole-cell neuronal electrical activity was carried out in Matlab (MATLAB Release 2015a, The Mathworks Inc., Natick, Massachusetts, US) using the following Hodgkin-Huxley formalism (Hodgkin and Huxley 1952). In particular, we use the following formulation for the ion-channel currents:

$$I = g_{max} * (m^P * h^Q) * (V - E)$$

$$\frac{dx}{dt} = \frac{x_\infty - x}{\tau_x}$$

$$x_\infty = \frac{1}{1 + e^{-\frac{V - V_h}{k}}}$$

$$\tau_x = Amp * e^{-\frac{V-V_{max}}{\sigma}}$$

where g_{max} denotes the maximum conductance, and x the state of the activation m and inactivation h gates respectively. The above formulation also includes the driving force, which is the difference between the membrane voltage, V, and the reversal potential, E. The reversal potentials were calculated using the Nernst equation based on the electrophysiological solutions used as 52 mV for sodium, -90 mV for potassium, and 132 mV for calcium. The steady-state of the gating variable x_∞ and the time-constant τ_x are calculated using parameters unique to each channel (see Table 1). These parameters have been determined by fitting to voltage-clamp experimental data in the same manner as originally done in (Hodgkin and Huxley 1952). The resulting current-balance equation describing the evolution of the whole cell membrane potential is:

$$C\frac{dV}{dt} = I_{app} - g_{Na}m^3h(V - E_{Na}) - g_{Ca}mh(V - E_{Ca}) - g_{Kv1}m^4h(V - E_K) - g_{Kv2}m^4(V - E_K)$$
$$- g_{Kv3}m^4h(V - E_K) - g_{Kv4}m^4h(V - E_K) - g_{leak}(V - E_{leak})$$

This equation includes the capacitance of the cell body, C (set at 3.7 pF in accordance with our recordings), along with the applied current, I$_{app}$, and the currents of the sodium, calcium, potassium, and leak channels to calculate the change in the membrane voltage, V. The sodium, calcium, and leak channel models are used unaltered from the previous Sim-Forger model (Sim and Forger 2007). Whole cell activity simulations are performed using the stochastic Euler-Maruyama method to iteratively calculate the membrane voltage incorporating white noise as follows:

$$V_{n+1} = V_n + \frac{dV_n}{dt}\Delta t + (\sigma W\sqrt{\Delta t})$$

Where V_n is the membrane voltage, dV_n/dt is the change in membrane voltage as calculated by the current-balance equation, $\Delta t = T/N$ is the time-step, T is the total simulation time,

$n = 1, \dots, N$ denotes the number if iterations, W is the white noise component, and σ is a scaling factor for the noise magnitude.

Electrophysiological data for the Kv channels Shaker, Shab, Shaw, and Shal were fit to Hodgkin-Huxley equations by standard Hill climbing (or direct search) search-based optimization algorithms (Kolda et al. 2003) to generate parameters describing kinetics of each individual ion channel. The parameters estimated for the four potassium channels and used in the dynamic clamp experiments are shown in Table 1.

Experimental design and statistical analysis

The liquid junction potential of the recordings was calculated as 13 mV and was subtracted from all the membrane voltages presented here. All values are given as mean and standard deviation (SD). Statistical tests were performed in Matlab (MATLAB Release 2015a, The MathWorks Inc., Natick, Massachusetts, US) or Prism (GraphPad Software Inc., La Jolla, CA, USA). A one-way ANOVA followed by Tukey's *post-hoc* test was used for circadian current data (Figures 1 and 3), Mantel-Cox log-rank test (Clark et al. 2003) for longevity data (Figure 4E) and a two-way ANOVA for the model-experimental firing rate comparisons (Figure 5C). For dynamic clamp channel experiments (Figures 6) equal variance is not assumed. A standard t-test was used for all other data after testing for a standard distribution with the Kolmogorov-Smirnoff test.

Code accessibility

Matlab codes utilized in the modelling and Signal scripts used for dynamic clamp are available upon request.

Results

Circadian changes in Shaw and Shal channel function

To determine the functional properties of Shaker, Shab, Shaw and Shal across the day, we examined the electrophysiological properties of the LNvs by whole-cell patch-clamp. Each channel was isolated by the use of ion channel specific pharmacological blockers: α-dendrotoxin (DTX, 100 nM) to block Shaker (Grissmer et al. 1994), guangxitoxin-1E (GxTX, 20 nM) to block Shab (Herrington et al. 2006), blood depressing substance (BDS-I, 300 nM) to block Shaw (Yeung 2005), and phrixotoxin-1 (PaTX, 100 nM) to target Shal (Gasque et al. 2005). Whole-cell current densities in response to a voltage-clamp protocol were recorded before and after application of the appropriate channel toxin (Figure 1). The respective ion channel currents were then estimated by subtracting the currents recorded in these two conditions (Figure 1B). Importantly, each toxin was unable to affect whole-cell currents when the corresponding channel was functionally removed by either dominant negative (DN) or *RNAi* transgenes specific for each of the individual Kv channels expressed in the LNvs (Figure 2A). This significant reduction in drug-sensitive current for each of Shaker ($t(22)=8.206$, $p<0.0001$, t-test), Shab ($t(22)=13.511$, $p<0.0001$, t-test), Shaw ($t(22)=2.765$, $p=0.0113$, t-test), and Shal ($t(22)=3.8764$, $p=0.0008$, t-test) demonstrates selectivity at their respective concentrations. The corresponding currents of each channel were also mostly restored by wash-out of the toxins (Figures 1D and 2B).

Each of the assayed Kv channels displayed characteristic kinetics in response to a voltage-clamp protocol (Tsunoda and Salkoff 1995; Gasque et al. 2005) (Figure 1C). Analysing the peak current density evoked by the highest depolarizing step at different times-of-day (Figure 1A) showed a consistent response for Shaker and

Shab, whereas Shaw ($F_{(3,8)}$=16.43, p=0.0009, one-way ANOVA) and Shal ($F_{(3,8)}$=9.36, p=0.0054, one-way ANOVA) varied across the day. Shaw displayed a higher peak current density in the morning (Zeitgeber time (ZT)2) compared with the night (ZT14) ($t_{(4)}$=11.406, p=0.0003, t-test). Conversely, Shal conducted a higher peak current density in the evening (ZT8) than at late night near dawn (ZT20) ($t_{(4)}$=11.429, p=0.0003, t-test).

To examine whether these changes in peak currents are of circadian origin or a consequence of light input, we recorded Shaw and Shal currents on the third day of DD in both l-LNvs and s-LNvs (Figure 3), as molecular oscillations in the l-LNvs dampens by then in DD, while remaining sustained in the s-LNvs (Yang and Sehgal 2001). Recordings in the s-LNvs exhibited oscillations in Shaw ($F_{(1,4)}$=12.89, p=0.0229, one-way ANOVA) and Shal ($F_{(1,4)}$=96.43, p=0.0006, one-way ANOVA) current density (Figure 3B) that were consistent with those obtained in LD (Figure 3A). However, corresponding recordings in the l-LNvs in DD (Figure 3B) showed reduced currents in both Shaw ($F_{(1,4)}$=0.07, p=0.7982, one-way ANOVA) and Shal ($F_{(1,4)}$=0.83, p=0.4149, one-way ANOVA) and abolished this rhythm. This is likely due to the disruption of the molecular clock observed after a transition from LD to DD. In *Drosophila* the molecular clock is dependent on the heterodimeric bHLH-PAS transcription factors CLOCK (CLK) or CYCLE (CYC), therefore clock neuron expression of DN transgenes to CLK and CYC results in completely arrhythmic flies under DD conditions and loss of rhythmic expression of timeless (tim) driven luciferase expression and rhythmic expression of tim mRNA at ZT9, ZT15 and ZT21 (Tanoue et al., 2004). Therefore, we recorded Shaw and Shal currents in flies expressing CLOCK (CLK) or CYCLE (CYC) DN transgenes in the LNvs (Figure 3C), which block the function of these core clock proteins and thus stops the molecular

clock. Interestingly, when CLK or CYC DN transgenes are expressed only in the LNvs the rhythm of Shaw and Shal is abolished even in LD conditions (Figure 3C). These results showed that the observed variations of Shaw and Shal currents were driven by the molecular clock.

Shaw and Shal currents affected circadian locomotor behavior and longevity

The behavioral consequences of disrupting the rhythm of Shaw and Shal currents were examined by assaying circadian behavior and longevity of flies expressing either Shaw or Shal DN transgenes in the LNvs (Figure 4). Locomotor behavior showed significant increases in overall activity (Figures 4A and D), particularly at night-time, when either Shaw ($t(27)=-6.5263$, $p<0.0001$, t-test) or Shal ($t(39)=-4.4307$, $p<0.0001$, t-test) channels are blocked. However, despite the increase in activity, the period (Figure 4C, Shaw: $t(27)=-5.878$, $p<0.0001$, Shal: $t(39)=1.163$, $p=0.2518$) and strength of the rhythms (Figure 4B, Shaw: $t(27)=2.003$, $p=0.0554$, Shal: $t(39)=0.1251$, $p=0.9011$) are not generally affected other than a small period lengthening seen with Shaw DN in DD. Interestingly, the longevity of flies expressing either Shaw ($p<0.0001$, Mantel-Cox) or Shal ($p<0.0001$, Mantel-Cox) DN in only the LNvs was significantly reduced compared to controls (Figure 4E).

Computational modeling of the circadian neurons

In order to determine the contribution of the observed oscillations in Shaw and Shal to the day-night rhythms of activity seen in clock neurons, we developed a computational model describing the kinetics of each Kv channel utilizing the LNv electrophysiological data, and tested it using dynamic clamp. The individual currents' models were parameterized by fitting the experimental data to Hodgkin-Huxley equations (Hodgkin and Huxley 1952), one of the most commonly used biophysical frameworks for studying ion channel activity that have already been used to model

the SCN (Sim and Forger 2007) and *Drosophila* DN1s (Flourakis et al. 2015) (Table 1). These Kv channel models were combined with a previously existing model of mammalian SCN sodium and calcium channels (Sim and Forger 2007) to produce a whole-cell neuronal model that described the LNv electrical activity.

Simulations of whole-cell electrical activity in this model reproduced the experimental observations of the LNvs (Figures 5A). Interestingly, the model only incorporated a time-of-day variation in Shaw and Shal conductance, while keeping Shaker and Shab constant, indicating that the former channels accounted for the day-night difference in electrical activity. During the simulation of individual action potentials, the current of the channels can also be observed. This revealed that Shaw and Shal were also preferentially active during the action potential in the morning and evening respectively (Figure 5B). We further analyzed our model in terms of spontaneous action potential firing frequency and found that it faithfully reproduced the difference in morning/evening firing rate (Figure 5C).

The availability of electrophysiological data and the construction of channel models allowed us to employ a dynamic clamp approach to study the behavior of the LNvs facilitated by real-time modulation of their electrical activity. First, to validate the channel models in an experimental setting, each voltage-gated potassium channel was separately blocked by their respective drugs (Figure 6). In current clamp, this produced a noticeable change in action potential firing rate (Figures 6A middle traces). The electrical activity was then rescued by injecting the calculated current (Figures 6A right traces), based on the respective channel model, and in real time using dynamic clamp (conductances used in Table 2). The firing rate (Figure 6B) changed on application of the drug (Shaker: $t(4.8)=-6.5493$, $p=0.0014$, Shab: $t(5.5)=-3.2578$, $p=0.0197$, Shaw: $t(5.7)=3.6298$, $p=0.012$, Shal: $t(7.8)=-7.3673$, $p<0.0001$)

and was rescued in all cases by application of the model (Shaker: t(6.8)=5.6572, p=0.0008, Shab: t(4.1)=3.9641, p=0.0159, Shaw: t(6.7)=-4.5437, p=0.003, Shal: t(6.5)=9.1094, p<0.0001). This affirms that the channel models described sufficiently well the channel kinetics and can substitute for the function of the actual channels in regulating electrical activity.

Since the computational model can also recapitulate the change in electrical activity between morning and evening states, we used the dynamic clamp set-up to modulate the activity of the LNvs (Figure 7 and Table 3). Addition of Shaw current and removal of Shal current using dynamic clamp caused a reduction in firing rate of the LNvs at ZT0 from the morning level of ~2 Hz to an evening level of ~1 Hz (t(6)=8.9324, p<0.0001) (Figures 7A left panel). Removal of Shaw current and addition of Shal current in contrast caused the converse effect on the LNvs at ZT12 shifting them from an evening level to a morning level of activity (t(4)=-10.6904, p<0.0001) (Figures 7A right panel). In other words, we were able to effectively switch a morning cell to an evening cell and vice versa (Figure 7B). Taken together our modeling confirmed that Shaw and Shal currents are sufficient to account for the day-night variation in electrical activity.

Discussion

In this study we identified the voltage-gated potassium channels Shaw and Shal as major contributors to the circadian changes in electrical activity of LNv clock neurons. Previous work has shown that the spontaneous action potential firing rate (e.g. ZT1-3: 2Hz and ZT13-15: 0.5Hz) and resting membrane potential (e.g. ZT1-3: -50mV and ZT13-15: -58 mV) of the LNvs changed over the day (Cao and Nitabach 2008; Sheeba et al. 2008; Buhl et al. 2016). However, the specific ion currents that underpinned rhythms of neuronal excitability were not known. Here we showed that

the currents of individual voltage-gated potassium channels, as revealed by selective blockers, displayed circadian variation (Figure 1). This variation persisted in DD but was abolished when the molecular clock was stopped (Figure 3) indicating that the variation in ion channel currents required a functional core molecular clock. Conversely, the disruption of the channels just in the LNv resulted in changes in circadian locomotor activity and decreased lifespan (Figure 4), showing the importance of circadian changes in clock neuron excitability and the behavioral rhythms they drive to the health span of an individual. Taken together, this positions the oscillation of Shaw and Shal currents as critical components of the molecular machinery in the membrane that regulates rhythmic changes in clock neuronal activity. We also implemented a dynamic clamp methodology, in *Drosophila* and for clock neurons for the first time and showed how the above findings can be utilized by computational modeling and dynamic clamp to modulate neuronal activity in real-time in order to switch between morning and evening states (Figure 7).

The circadian rhythm of Shaw and Shal currents observed here may be generated by a number of processes. A previous transcriptomic study (Kula-Eversole et al. 2010) indicated that the mRNA levels of both channels cycle in a circadian manner in the LNvs with Shaw being highest in the morning and Shal being highest in the evening, and so the changes in current could be underpinned by changes in transcription. Indeed, studies in the SCN also report circadian variation in the Shal ortholog Kv4.1, its knock-down had a greater effect at night (Hermanstyne et al. 2017) with similar effects reported in *Drosophila* (Feng et al. 2018). While neither Shaw nor Shal genes contain a canonical E-box sequence (Nakahata et al. 2008), many genes found to have a cycling mRNA level do not contain known circadian transcription elements (Claridge-Chang et al. 2001; McDonald and Rosbash 2001).

Furthermore, many rhythmic proteins found in the mouse liver and SCN have been shown not to be encoded by rhythmic mRNAs (Mauvoisin et al. 2014; Robles et al. 2014). Therefore, studies at the protein and functional level are more reliable, in this case the functional assay for ion channels is electrophysiology. In the SCN, Kv3 showed higher expression during the day (Itri et al. 2005). It is, however, interesting that disruption of the molecular clock led to, not only an abolition of the Shaw and Shal current cycling, but also an abolition of Shaw and Shal current in general (Figure 3C). This suggests that, while circadian transcription of specific channels maybe unclear, the molecular clock seems necessary for the rhythmic timing of membrane properties of clock neurons. Indeed, circadian expression and degradation of clock neuron ion channels may not be the most parsimonious means to circadianly regulate membrane properties, for instance post-transcriptional modifications have also been found to be important (Ko et al. 2009). In addition, alternative splicing is important for changing ion channel function, especially for voltage-gated potassium channels (Jan and Jan 2012), with *Drosophila* ion channels such as Shaker and Shab that are expressed in clock neurons can also undergo RNA editing (Ingleby et al. 2009; Ryan et al. 2008). Furthermore, a recent study showed that potassium channels were the most alternatively spliced gene family in the genome, with alternative splicing transcripts (especially Shaker and Shab) being particularly enriched in LNv and DN1 compared to non-circadian neurons. It is not known if or how this massive alternative splicing regulation of clock neurons contributes to circadian rhythms (Wang et al. 2018).

A study of the *Drosophila* dorsal clock neurons identified that localization of the sodium channel NA is important for circadian changes in electrical activity (Flourakis et al. 2015). Here, RNA-seq analysis showed no cycling of *NA* transcripts, but

instead showed rhythms in the localization factor *NLF-1*. The mammalian ortholog of NA, termed NALCN, showed similar rhythms suggesting conservation between flies and mammals. Voltage-gated potassium channels, such as Shaker, have also been shown to interact with accessory subunits such as Hyperkinetic with both being shown to be important for *Drosophila* sleep and longevity, with null mutants sleeping a third as long as normal flies resulting in flies with significant reductions in lifespan (Bushey et al. 2007; Cirelli et al. 2005; Kempf et al. 2019). Phosphorylation may also be an important post-translational means of circadian regulation of ion channel activity, with mammalian slo or BK, being under phosphorylation control in the SCN (Shelley et al. 2013). Circadian phosphorylation by clock kinases maybe a more general bi-directional link between the molecular clock and membrane ion channels that regulate the rhythmic firing of clock neurons (Ko et al. 2009; Allada and Chung 2010; Allen et al. 2017).

Membrane activity of the LNvs has been previously suggested to be particularly important for self-sustained oscillations as electrical silencing of the LNvs stopped the molecular clock (Nitabach et al. 2002; Depetris-chauvin et al. 2011). Additionally, hyperexcitation of the LNvs has been reported to create a shift in the transcriptome towards a morning-like state whereas hyperpolarization shifts towards an evening-like state (Mizrak et al. 2012; Emery 2012). This link between the molecular clock and the rhythmic changes in the membrane excitability could also relate (at least in part) to the ion channels Shaw and Shal themselves as proposed above and via membrane potential control of neurotransmitter and peptide release (Choi et al. 2012).

PDF is known to rhythmically accumulate in the dorsal terminals of the s-LNvs with more PDF during the day than at night (Park et al. 2000). Previous reports (Hodge

and Stanewsky 2008) indicate that expression of the *Shaw DN* transgene throughout the *Drosophila* clock network results in lower PDF levels in the terminals across the day with a reduced strength of oscillation, presumably due to reduced Shaw causing depolarization of terminals and PDF release. The opposite effect is seen with over-expression of Shaw resulting in increased Shaw-mediated hyperpolarization and block of calcium-mediated exocytosis and therefore an increase in overall PDF levels in the terminals and a loss of rhythm. Taken together this indicates that reduction of Shaw function leads to a lower level of PDF, and hence changes in PDF signaling, possibly underlying effects observed here in altering circadian locomotor activity (Figure 4).

The increased activity and reduced sleep associated with altering Shaw and Shal currents (Figure 4A-D) indicate a hyperactive behavioral phenotype. The increase in locomotor activity is particularly pronounced in night-time activity, consistent with the role of the l-LNvs as wake-promoting neurons (Parisky et al. 2008) and with previous reports of the role of Shaw (Hodge and Stanewsky 2008) and Shal (Feng et al. 2018) in circadian behavior. The decrease in lifespan seen by disrupting either Shaw or Shal (Figure 4E) also mirrors other studies showing that loss of Shaker or Shal throughout the brain leads to a shortening of lifespan (Ping et al. 2011; Bushey et al. 2007). However, our study extends these findings, by demonstrating that the mechanism by which the reduction in lifespan can occur is by disruption of circadian rhythms caused by the loss of specific voltage-gated potassium channels just in the LNvs. In humans, a related disease is Morvan's syndrome whereby antibodies are produced against the Kv1 channel and result in loss of sleep and increased mortality (Irani et al. 2010). Mutation in human Kv9, which co-assembles with Kv2, has similarly been shown to be associated with essential tremor and when expressed in

Drosophila clock neurons results in hyperexcitability, loss of night-time sleep, shaking and increased mortality (Smith et al. 2018).

The combination of electrophysiology and computational modeling enabled us to employ dynamic clamp in order to directly test whether changes in Shaw and Shal currents are sufficient to recapitulate changes in electrical activity (Figure 7). The dynamic clamp technique allows us to simulate the presence or absence of a channel, by injecting appropriate current based on its mathematical model in real time (Prinz et al. 2004; Goaillard and Marder 2006). This approach reinforces the capability of these ion channels to generate the specific patterns of electrical activity observed, such as action potential firing frequency, by showing that changes only in these ion channels recreate this phenomenon.

The kinetics of Shaw (Kv3) and Shal (Kv4) channels seem particularly well suited for modulating the firing rate with Shal mediating the fast transient I_A current necessary for rapid repolarization of action potentials required for high frequency firing and the delay to the first spike in a burst of action potentials of a range of *Drosophila* neurons including clock neurons (Feng et al., 2018; Hodge et al., 2005; Kulik et al., 2019; Ping et al., 2011). Kv4 also mediates the I_A current in a range of mammalian neurons including in the SCN thereby regulating spike timing, repetitive firing, spontaneous firing, dendritic integration and plasticity and has been shown to be able to tune pacemaker frequency of action potentials (Amarillo et al., 2008; Hermanstyne et al., 2017; Liss et al., 2001). On the other hand, Shaw regulates the firing rate in a range of *Drosophila* neurons including clock neurons probably by a separate mechanism to Shal, via controlling the resting membrane potential (Buhl et al., 2016; Hodge et al., 2005; Tsunoda and Salkoff, 1995). Interestingly, the duplication of the Shaw gene in mammals has created a diversity of Kv3 channels, some of which have particularly

fast kinetics that can adjust and maintain firing rates of neurons such as in the auditory system up to around 200 Hz (Rudy and McBain, 2001; Wang et al., 1998). Kv3 channels also control spike timing, spontaneous firing and firing patterns in a range of other neurons including in the SCN (Akemann and Knopfel, 2006; Joho et al., 2006; Kudo et al., 2011; Kudo et al., 2013). In future, the model we developed could, alongside other similar models (Flourakis et al. 2015), contribute to a larger model encapsulating how different orthologues of the same channel in clock neurons of different species result in their respective firing behavior or how the different ion channels contribute to the firing properties of different types of neurons in the same species, for instance neurons from different clock groups or even describe the clock network at large and the role of rhythmic changes in membrane properties to the clock and its function. Investigating the interaction of Shaw and Shal potassium with the NA sodium currents and the rescue of neuronal activity rhythms using dynamic clamp, will help us to understand the possible cooperation between different ion channels in regulating rhythmic activity. In addition, this model reiterates the conservation between *Drosophila* and mammalian clock neuron excitability and circadian rhythms and their importance in health and disease and potential of applications to chronotherapy (Allen et al. 2017; Julienne et al. 2017; Zwarts et al. 2017).

In conclusion, we demonstrate that the voltage-gated potassium channels Shaw and Shal exhibit circadian changes in their current profile within the LNv clock neurons and that these rhythmic changes in membrane excitability have real consequences for the animal. We built computational models that describe how these changes affect whole-cell electrophysiology and indicate the importance of these channel oscillation for functional day-night differences. Finally, by using dynamic clamp we

could verify our models and were able to switch the neurons between morning- and evening-like electrical states.

Author contributions: P.S. conducted the experiments and wrote the paper, E.B. developed novel technology for the project, supervised project and edited the paper, K.A.-T. and J.H. secured funding, designed experiments, supervised project and edited the paper.

Competing interest: Authors report no competing interests.

References

Akemann, W. and Knopfel, T. (2006). Interaction of Kv3 potassium channels and resurgent sodium current influences the rate of spontaneous firing of Purkinje neurons. *J Neurosci* 26, 4602-4612.

Allada, R. and Chung, B.Y., (2010) Circadian Organization of Behavior and Physiology in *Drosophila*. *Neurobiology*, pp.605–624.

Allen, C.N., Nitabach, M.N., and Colwell, C.S., (2017) Membrane Currents, Gene Expression, and Circadian Clocks. *Cold Spring Harbor perspectives in biology*, 9(5).

Amarillo, Y., De Santiago-Castillo, J.A., Dougherty, K., Maffie, J., Kwon, E., Covarrubias, M., and Rudy, B. (2008). Ternary Kv4.2 channels recapitulate voltage-dependent inactivation kinetics of A-type K+ channels in cerebellar granule neurons. *J Physiol* 586, 2093-2106.

Belle, M.D.C., Diekman, C.O., Forger, D.B., and Piggins, H.D., (2009) Daily electrical silencing in the mammalian circadian clock. *Science*, 326(5950), pp.281–284.

Belle, M.D.C., and Allen, C.N. (2018). The circadian clock: A tale of genetic-electrical interplay and synaptic integration. Current opinion in physiology *5*, 75-79.

Buhl, E., Bradlaugh, A., Ogueta, M., Chen, K.-F., Stanewsky, R., and Hodge, J.J.L., (2016) Quasimodo mediates daily and acute light effects on *Drosophila* clock neuron excitability. *Proceedings of the National Academy of Sciences*, 113(47), pp.13486–13491.

Bushey, D., Huber, R., Tononi, G., and Cirelli, C., (2007) *Drosophila* Hyperkinetic Mutants Have Reduced Sleep and Impaired Memory. *Journal of Neuroscience*, 27(20), pp.5384–5393.

Cao, G. and Nitabach, M.N., (2008) Circadian control of membrane excitability in *Drosophila* melanogaster lateral ventral clock neurons Guan. *J Neurosci*, 19(25), pp.389–399.

Chen, C., Buhl, E., Xu, M., Croset, V., Rees, J.S., Lilley, K.S., Benton, R., Hodge, J.J.L., and Stanewsky, R., (2015) *Drosophila* Ionotropic Receptor 25a mediates circadian clock resetting by temperature. *Nature*, 527(7579), pp.516–520.

Choi, C., Cao, G., Tanenhaus, A.K., McCarthy, E. v., Jung, M., Schleyer, W., Shang, Y., Rosbash, M., Yin, J.C.P., and Nitabach, M.N., (2012) Autoreceptor Control of Peptide/Neurotransmitter Corelease from PDF Neurons Determines Allocation of Circadian Activity in *Drosophila*. *Cell Reports*, 2(2), pp.332–344.

Cirelli, C., Bushey, D., Hill, S., Huber, R., Kreber, R., Ganetzky, B., and Tononi, G., (2005) Reduced sleep in *Drosophila* Shaker mutants. *Nature*, 434(7037), pp.1087–1092.

Claridge-Chang, A, Wijnen, H., Naef, F., Boothroyd, C., Rajewsky, N., and Young, M.W., (2001) Circadian regulation of gene expression systems in the *Drosophila* head. *Neuron*, 32(4), pp.657–671.

Clark, T.G., Bradburn, M.J., Love, S.B., and Altman, D.G., (2003) Survival Analysis Part I: Basic concepts and first analyses. *British Journal of Cancer*, 89(2), pp.232–238.

Coetzee, W.A., Amarillo, Y., Chiu, J., Chow, A., Lau, D., McCormack, T., Morena, H., Nada, M.S., Ozaita, A., Pountney, D., Saganich, M., Miera, E.V.-S., and Rudy, B., (1999) Molecular Diversity of K+ Channels. *Annals of the New York Academy of Sciences*, 868, pp.233–255.

Colwell, C.S. (2011). Linking neural activity and molecular oscillations in the SCN. Nature reviews Neuroscience *12*, 553-569.

Depetris-chauvin, A., Berni, J., Aranovich, E.J., Muraro, N.I., Beckwith, J., and Ceriani, M.F., (2011) Adult-specific electrical silencing of pacemaker neurons uncouples the molecular oscillator from circadian outputs. *Curr Biol*, 21(21), pp.1783–1793.

Diekman, C.O., Belle, M.D.C., Irwin, R.P., Allen, C.N., Piggins, H.D., and Forger, D.B., (2013) Causes and Consequences of Hyperexcitation in Central Clock Neurons. *PLoS Computational Biology*, 9(8).

Emery, P., (2012) Circadian rhythms: An electric jolt to the clock. *Current Biology*, 22(20), pp.R876–R878.

Feng, G., Zhang, J., Li, M., Shao, L., Yang, L., Song, Q., and Ping, Y., (2018) Control of sleep onset by Shal/K $_v$ 4 channels in *Drosophila* circadian neurons. *The Journal of Neuroscience*, pp.0777-18.

Flourakis, M., Kula-Eversole, E., Hutchison, A.L., Han, T.H., Aranda, K., Moose, D.L., White, K.P., Dinner, A.R., Lear, B.C., Ren, D., Diekman, C.O., Raman, I.M., and Allada, R., (2015) A Conserved Bicycle Model for Circadian Clock Control of Membrane Excitability. *Cell*, 162(4), pp.836–848.

Fogle, K.J., Baik, L.S., Houl, J.H., Tran, T.T., Roberts, L., Dahm, N.A., Cao, Y., Zhou, M., and Holmes, T.C. (2015). CRYPTOCHROME-mediated phototransduction by modulation of the potassium ion channel beta-subunit redox sensor. *Proceedings of the National Academy of Sciences of the United States of America* 112, 2245-2250.

Gasque, G., Labarca, P., Reynaud, E., and Darszon, A., (2005) Shal and Shaker Differential Contribution to the K+ Currents in the *Drosophila* Mushroom Body Neurons. *Journal of Neuroscience*, 25(9), pp.2348–2358.

Goaillard, J.-M. and Marder, E., (2006) Dynamic Clamp Analyses of Cardiac, Endocrine, and Neural Function. *Physiology*, 21(3), pp.197–207.

Granados-Fuentes, D., Hermanstyne, T.O., Carrasquillo, Y., Nerbonne, J.M., and Herzog, E.D. (2015). IA Channels Encoded by Kv1.4 and Kv4.2 Regulate Circadian Period of PER2 Expression in the Suprachiasmatic Nucleus. *J Biol Rhythms* 30, 396-407.

Granados-Fuentes, D., Norris, A.J., Carrasquillo, Y., Nerbonne, J.M., and Herzog, E.D. (2012). IA Channels Encoded by Kv1.4 and Kv4.2 Regulate Neuronal Firing in the Suprachiasmatic Nucleus and Circadian Rhythms in Locomotor Activity. *Journal of Neuroscience* 32, 10045-10052.

Grissmer, S., Nguyen, A., Aiyar, J., Hanson, D., Mather, R., Gutman, G., Karmilowicz, M., Auperin, D., and Chandy, K., (1994) Pharmacological Characterization of Five Cloned Voltage-Gated Expressed in Mammalian Cell Lines. *Molecular Pharmacology*, 45, pp.1227–1234.

Hablitz, L.M., Molzof, H.E., Paul, J.R., Johnson, R.L., and Gamble, K.L. (2014). Suprachiasmatic nucleus function and circadian entrainment are modulated by G protein-coupled inwardly rectifying (GIRK) channels. The Journal of physiology *592*, 5079-5092.

Helfrich-Förster, C., Stengl, M., and Homberg, U., (1998) Organization of the circadian system in insects. *Chronobiology International*, 15(6), pp.567–594.

Helfrich-Förster, C., Yoshii, T., Wülbeck, C., Grieshaber, E., Rieger, D., Bachleitner, W., Cusumano, P., and Rouyer, F., (2007) The lateral and dorsal neurons of *Drosophila* melanogaster: New insights about their morphology and function. *Cold Spring Harbor Symposia on Quantitative Biology*, 72, pp.517–525.

Hermanstyne, T.O., Granados-Fuentes, D., Mellor, R.L., Herzog, E.D., and Nerbonne, J.M., (2017) Acute Knockdown of Kv4.1 Regulates Repetitive Firing Rates and Clock Gene Expression in the Suprachiasmatic Nucleus and Daily Rhythms in Locomotor Behavior. *Eneuro*, 4(June), p.ENEURO.0377-16.2017.

Herrington, J., Zhou, Y.P., Bugianesi, R.M., Dulski, P.M., Feng, Y., Warren, V.A., Smith, M.M., Kohler, M.G., Garsky, V.M., Sanchez, M., Wagner, M., Raphaelli, K., Banerjee, P., Ahaghotu, C., Wunderler, D., Priest, B.T., Mehl, J.T., Garcia, M.L., McManus, O.B., Kaczorowski, G.J., and Slaughter, R.S., (2006) Blockers of the delayed-rectifier potassium current in pancreatic β-cells enhance glucose-dependent insulin secretion. *Diabetes*, 55(4), pp.1034–1042.

Hodge, J.J. and Stanewsky, R., (2008) Function of the Shaw potassium channel within the *Drosophila* circadian clock. *PLoS ONE*, 3(5).

Hodge, J.J.L., Choi, J.C., O'Kane, C.J., and Griffith, L.C., (2005) Shaw potassium channel genes in *Drosophila*. *Journal of Neurobiology*, 63(3), pp.235–254.

Hodgkin, A.L. and Huxley, A.F., (1952) A quantitative description of membrane current and its application to conduction and excitation in nerve. *Bulletin of Mathematical Biology*, 52(1–2), pp.25–71.

Ingleby, L., Maloney, R., Jepson, J., Horn, R., and Reenan, R., (2009) Regulated RNA editing and functional epistasis in Shaker potassium channels. *The Journal of general physiology*, 133(1), pp.17–27.

Irani, S.R., Alexander, S., Waters, P., Kleopa, K.A., Pettingill, P., Zuliani, L., Peles, E., Buckley, C., Lang, B., and Vincent, A., (2010) Antibodies to Kv1 potassium channel-complex proteins leucine-rich, glioma inactivated 1 protein and contactin-associated protein-2 in limbic encephalitis, Morvan's syndrome and acquired neuromyotonia. *Brain*, 133(9), pp.2734–2748.

Itri, J.N., Michel, S., Vansteensel, M.J., Meijer, J.H., and Colwell, C.S., (2005) Fast Delayed Rectifier Potassium Current Required for Circadian Neural Activity. *Nat Neurosci*, 8(5), pp.650–656.

Itri, J.N., Vosko, A.M., Schroeder, A., Dragich, J.M., Michel, S., and Colwell, C.S., (2010) Circadian Regulation of A-Type Potassium Currents in the Suprachiasmatic Nucleus. *Journal of Neurophysiology*, 103(2), pp.632–640.

Jan, L.Y. and Jan, Y.N., (2012) Voltage-gated potassium channels and the diversity of electrical signalling. *The Journal of physiology*, 590(11), pp.2591–2599.

Joho, R.H., Marks, G.A., and Espinosa, F. (2006). Kv3 potassium channels control the duration of different arousal states by distinct stochastic and clock-like mechanisms. *The European journal of neuroscience* 23, 1567-1574.

Julienne, H., Buhl, E., Leslie, D.S., and Hodge, J.J.L., (2017) *Drosophila* PINK1 and parkin loss-of-function mutants display a range of non-motor Parkinson's disease phenotypes.

Neurobiology of Disease, 104, pp.15–23.

Kempf, A., Song, S.M., Talbot, C.B., and Miesenböck, G. (2019). A potassium channel β-subunit couples mitochondrial electron transport to sleep. *Nature* 568, 230-234.

Kent, J., and Meredith, A.L. (2008). BK channels regulate spontaneous action potential rhythmicity in the suprachiasmatic nucleus. PloS one *3*, e3884.

Ko, G.Y.-P., Shi, L., and Ko, M.L., (2009) Circadian regulation of ion channels and their functions. *Journal of neurochemistry*, 110(4), pp.1150–1169.

Kolda, T., Lewis, R., and Torczon, V., (2003) Optimization by Direct Search: New Perspectives on Some Classical and Modern Methods. *SIAM Review*, 45(3), pp.385–482.

Kudo, T., Loh, D.H., Kuljis, D., Constance, C., and Colwell, C.S., (2011) Fast delayed rectifier potassium current: critical for input and output of the circadian system Takashi. *J Neurosci*, 31(8), pp.2746–55.

Kudo, T., Tahara, Y., Gamble, K.L., McMahon, D.G., Block, G.D., and Colwell, C.S. (2013). Vasoactive intestinal peptide produces long-lasting changes in neural activity in the suprachiasmatic nucleus. *J Neurophysiol* 110, 1097-1106.

Kula-Eversole, E., Nagoshi, E., Shang, Y., Rodriguez, J., Allada, R., and Rosbash, M., (2010) Surprising gene expression patterns within and between PDF-containing circadian neurons in *Drosophila*. *Proceedings of the National Academy of Sciences*, 107(30), pp.13497–13502.

Kulik, Y., Jones, R., Moughamian, A.J., Whippen, J., and Davis, G.W. (2019). Dual separable feedback systems govern firing rate homeostasis. *Elife* 8.

Levine, J.D., Funes, P., Dowse, H.B., and Hall, J.C., (2002) Signal analysis of behavioral and molecular cycles. *BMC Neuroscience*, 3, pp.1–25.

Liss, B., Franz, O., Sewing, S., Bruns, R., Neuhoff, H., and Roeper, J. (2001). Tuning

pacemaker frequency of individual dopaminergic neurons by Kv4.3L and KChip3.1 transcription. *Embo j* 20, 5715-5724.

Mauvoisin, D., Wang, J., Jouffe, C., Martin, E., Atger, F., Waridel, P., Quadroni, M., Gachon, F., and Naef, F., (2014) Circadian clock-dependent and -independent rhythmic proteomes implement distinct diurnal functions in mouse liver. *Proceedings of the National Academy of Sciences*, 111(1), pp.167–172.

McDonald, M.J. and Rosbash, M., (2001) Microarray analysis and organization of circadian gene expression in *Drosophila*. *Cell*, 107(5), pp.567–578.

McNally, B.A., Plante, A.E., and Meredith, A.L. (2019). Diurnal properties of voltage-gated Ca(2+) currents in suprachiasmatic nucleus and roles in action potential firing. *The Journal of physiology* DOI: 10.1113/JP278327.

Meijer, J.H., and Michel, S. (2015). Neurophysiological analysis of the suprachiasmatic nucleus: a challenge at multiple levels. *Methods in enzymology* 552, 75-102.

Meredith, A.L., Wiler, S.W., Miller, B.H., Takahashi, J.S., Fodor, A.A., Ruby, N.F., and Aldrich, R.W. (2006). BK calcium-activated potassium channels regulate circadian behavioral rhythms and pacemaker output. *Nature neuroscience* 9, 1041-1049.

Mizrak, D., Ruben, M., Myers, G.N., Rhrissorrakrai, K., Gunsalus, K.C., and Blau, J., (2012) Electrical activity can impose time of day on the circadian transcriptome of pacemaker neurons. *Current Biology*, 22(20), pp.1871–1880.

Nakahata, Y., Yoshida, M., Takano, A., Soma, H., Yamamoto, T., Yasuda, A., Nakatsu, T., and Takumi, T., (2008) A direct repeat of E-box-like elements is required for cell-autonomous circadian rhythm of clock genes. *BMC Molecular Biology*, 9, pp.1–11.

Nitabach, M.N., Blau, J., and Holmes, T.C., (2002) Electrical Silencing of *Drosophila* Pacemaker Neurons Stops the Free-Running Circadian Clock. *Cell*, 109, pp.485–495.

Nitabach, M.N., Holmes, T.C., and Blau, J. (2005). Membranes, ions, and clocks: testing the Njus-Sulzman-Hastings model of the circadian oscillator. Methods in enzymology *393*, 682-693.

Panda, S., Hogenesch, J.B., and Kay, S.A., (2002) Circadian rhythms from flies to human. *Nature*, 417(6886), pp.329–335.

Parisky, K.M., Agosto, J., Pulver, S.R., Shang, Y., Hodge, J.J.L., Kang, K., Liu, X., Garrity, P.A., and Griffith, L.C., (2008) PDF cells are a GABA-responsive wake-promoting component of the *Drosophila* sleep circuit Katherine. *Neuron*, 60(4), pp.672–682.

Park, J.H. and Hall, J.C., (1998) Isolation and Chronobiological Analysis of a Neuropeptide Pigment-Dispersing Factor Gene in *Drosophila melanogaster*. *Journal of Biological Rhythms*, 13(3), pp.219–228.

Park, J.H., Helfrich-Förster, C., Lee, G., Liu, L., Rosbash, M., and Hall, J.C., (2000) Differential regulation of circadian pacemaker output by separate clock genes in *Drosophila*. *Proc Natl Acad Sci U S A*, 97(7), pp.3608–3613.

Pennartz, C.M., de Jeu, M.T., Bos, N.P., Schaap, J., and Geurtsen, A.M. (2002). Diurnal modulation of pacemaker potentials and calcium current in the mammalian circadian clock. Nature *416*, 286-290.

Ping, Y., Waro, G., Licursi, A., Smith, S., Vo-Ba, D.A., and Tsunoda, S., (2011) Shal/Kv4 channels are required for maintaining excitability during repetitive firing and normal locomotion in *Drosophila*. *PLoS ONE*, 6(1), pp.15–20.

Prinz, A.A., Abbott, L.F., and Marder, E., (2004) The dynamic clamp comes of age. *Trends in Neurosciences*, 27(4), pp.218–224.

Robles, M.S., Cox, J., and Mann, M., (2014) In-Vivo Quantitative Proteomics Reveals a Key Contribution of Post-Transcriptional Mechanisms to the Circadian Regulation of Liver Metabolism. *PLoS Genetics*, 10(1).

Ruben, M., Drapeau, M.D., Mizrak, D., and Blau, J., (2012) A mechanism for circadian control of pacemaker neuron excitability Marc. , 27(5), pp.353–364.

Rudy, B. and McBain, C.J. (2001). Kv3 channels: voltage-gated K+ channels designed for high-frequency repetitive firing. *Trends in neurosciences* 24, 517-526.

Ryan, M.Y., Maloney, R., Reenan, R., and Horn, R., (2008) Characterization of five RNA editing sites in Shab potassium channels. *Channels (Austin, Tex.)*, 2(3), pp.202–209.

Schubert, F.K., Hagedorn, N., Yoshii, T., Helfrich-Förster, C., and Rieger, D., (2018) Neuroanatomical details of the lateral neurons of *Drosophila melanogaster* support their functional role in the circadian system. *Journal of Comparative Neurology*, 526(7), pp.1209–1231.

Sheeba, V., Fogle, K.J., Kaneko, M., Rashid, S., Chou, Y., and Vijay, K., (2008) Large Ventral Lateral Neurons Modulate Arousal and Sleep in *Drosophila*. *Curr Biol*, 18(20), pp.1537–1545.

Sheeba, V., Gu, H., Sharma, V.K., Dowd, D.K.O., and Todd, C., (2008) Circadian- and Light-Dependent Regulation of Resting Membrane Potential and Spontaneous Action Potential Firing of *Drosophila* Circadian Pacemaker Neurons. *J Neurophysiol*, 99(2), pp.976–988.

Shelley, C., Whitt, J.P., Montgomery, J.R., and Meredith, A.L., (2013) Phosphorylation of a constitutive serine inhibits BK channel variants containing the alternate exon 'SRKR'. *The Journal of general physiology*, 142(6), pp.585–598.

Sim, C.K. and Forger, D.B., (2007) Modeling the electrophysiology of suprachiasmatic nucleus neurons. *Journal of Biological Rhythms*, 22(5), pp.445–453.

Smith, P., Arias, R., Sonti, S., Odgerel, Z., Santa-Maria, I., McCabe, B.D., Tsaneva-Atanasova, K., Louis, E.D., Hodge, J.J.L., and Clark, L.N., (2018) A *Drosophila* Model of Essential Tremor. *Scientific reports*, 8(1), p.7664.

Taghert, P.H. and Shafer, O.T., (2006) Mechanisms of clock output in the *Drosophila* circadian pacemaker system. *Journal of Biological Rhythms*, 21(6), pp.445–457.

Tanoue, S., Krishnan, P., Krishnan, B., Dryer, S.E., and Hardin, P.E., (2004) Circadian Clocks in Antennal Neurons Are Necessary and Sufficient for Olfaction Rhythms in *Drosophila*. *Curr Biol*, 14(1), pp.638–49.

Tsunoda, S. and Salkoff, L., (1995) Genetic analysis of *Drosophila* neurons: Shal, Shaw, and Shab encode most embryonic potassium currents. *The Journal of Neuroscience*, 15(3), pp.1741–1754.

Wang, Q., Abruzzi, K.C., Rosbash, M., and Rio, D.C., (2018) Striking circadian neuron diversity and cycling of *Drosophila* alternative splicing. *eLife*, 7, pp.1–35.

Wang, L.Y., Gan, L., Forsythe, I.D., and Kaczmarek, L.K. (1998). Contribution of the Kv3.1 potassium channel to high-frequency firing in mouse auditory neurones. *J Physiol* 509, 183-194.

Whitt, J.P., Montgomery, J.R., and Meredith, A.L. (2016). BK channel inactivation gates daytime excitability in the circadian clock. *Nature communications* 7, 10837.

Wu, Y., Cao, G., and Nitabach, M.N., (2008) Electrical silencing of PDF neurons advances the phase of non-PDF clock neurons in *Drosophila*. *Journal of Biological Rhythms*, 23(2), pp.117–128.

Yang, Z. and Sehgal, A., (2001) Role of molecular oscillations in generating behavioral rhythms in *Drosophila*. *Neuron*, 29(2), pp.453–467.

Yeung, S.Y.M., (2005) Modulation of Kv3 Subfamily Potassium Currents by the Sea Anemone Toxin BDS: Significance for CNS and Biophysical Studies. *Journal of Neuroscience* 25(38), 8735–8745.

Zwarts, L., Vulsteke, V., Buhl, E., Hodge, J.J.L., and Callaerts, P., (2017) SlgA, encoded by the homolog of the human schizophrenia-associated gene PRODH, acts in clock

neurons to regulate *Drosophila* aggression. *Dis Model Mech*, 10(6) 705–16.

Figure legends

Figure 1: Daily changes in current profiles of voltage-gated potassium channels in l-LNvs.

A, Peak current density of each of the channels: Shaker (N=12), Shab (N=12), Shaw (N=13), and Shal (N=12) in the l-LNvs at different times of day in a 12 h:12 h light/dark cycle (LD). Shaker and Shab showed no significant changes over the day, whereas Shaw was highest in the morning (p=0.0003) and Shal was highest in the evening (p=0.0003). Asterisks indicate statistical significance throughout (*p<0.05, **p<0.01, ***p<0.001) in a one-way ANOVA, Tukey's *post-hoc* test. Box and whiskers are median, inter-quantile range (IQR) and minimum-maximum (min-max) throughout over four trials per time-point. **B,** Average current density profile of each individual channel in response to a voltage protocol shown in **C**, The presented profiles are the difference between control condition and after application of a selective blocker (Shaker: α-Dendrotoxin (DTX) 100 nM, Shab: Guangxitoxin-1E (GxTX) 20 nM, Shaw: blood-dispersing substance (BDS) 300 nM and Shal: Phrixotoxin-1 (PaTX) 100 nM). Shaker and Shab profiles were averages over the day, the Shaw profile was an average at ZT1-3, the Shal profile was an average at ZT7-9. **D,** A representative response to depolarization to -3 mV before (control) and after drug application (+DTX) as well as after a subsequent 5 minutes wash-out (after wash-out) that restored the blocked current. Similar wash-out experiments

were conducted for each of the channels Shaker, Shab, Shaw, and Shal and their respective blockers.
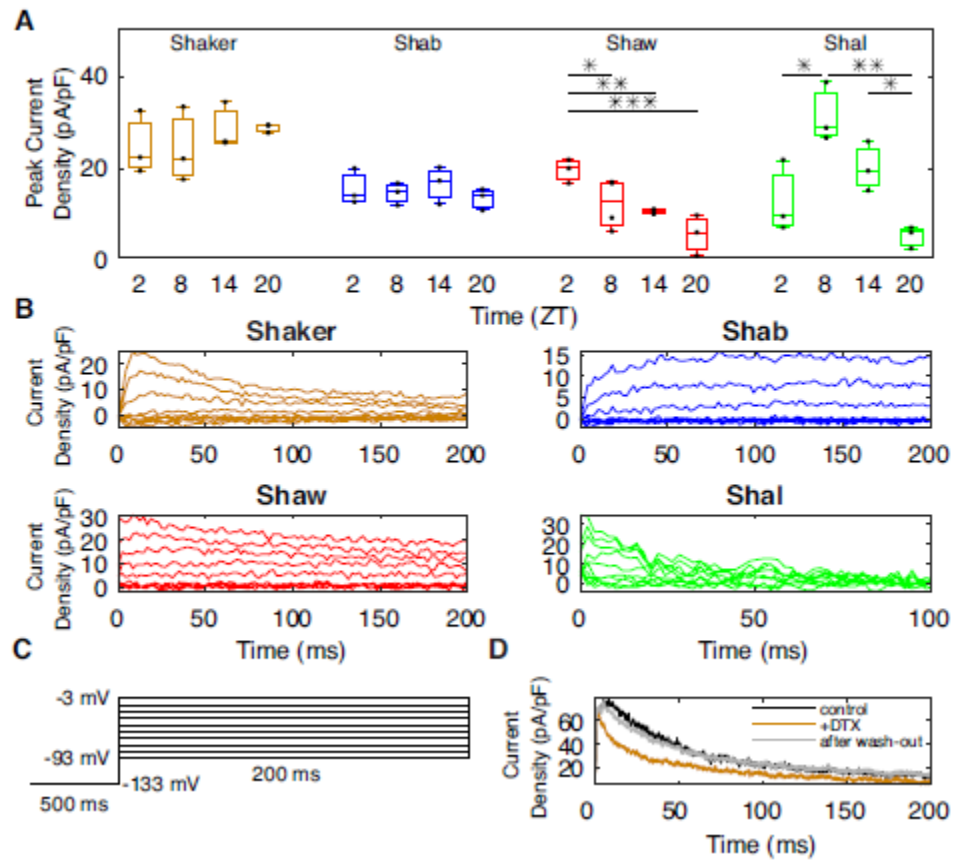
Figure 1

Figure 2: Validation of individual voltage-gated potassium channel blocker specificity in l-LNvs.

A, Peak current density blocked by ion channel blockers (Shaker: DTX, Shab: GxTX, Shaw: BDS, Shal: PaTX) on depolarization to -3 mV from -133 mV in l-LNvs of control flies (left colored boxes) or flies deficient for the corresponding channel (right black boxes). Shaker and Shab currents were obtained at ZT7-9 in control flies (n=12 and 12) and in *PDF-Gal4* driven expression of *Shaker RNAi* (n=9) or *Shab RNAi* (n=9). Shaw currents were obtained at ZT1-3 in controls (n=9) and l-LNvs expressing Shaw DN (n=9). Shal currents were obtained at ZT13-15 in controls (n=9) and l-LNvs expressing Shal DN (n=9). **B,** Percentage of blocked current that was recovered upon wash-out of the drug over 5 minutes for each ion channel. Box and whiskers are median, IQR and min-max over three trials per drug (n=3 per drug).
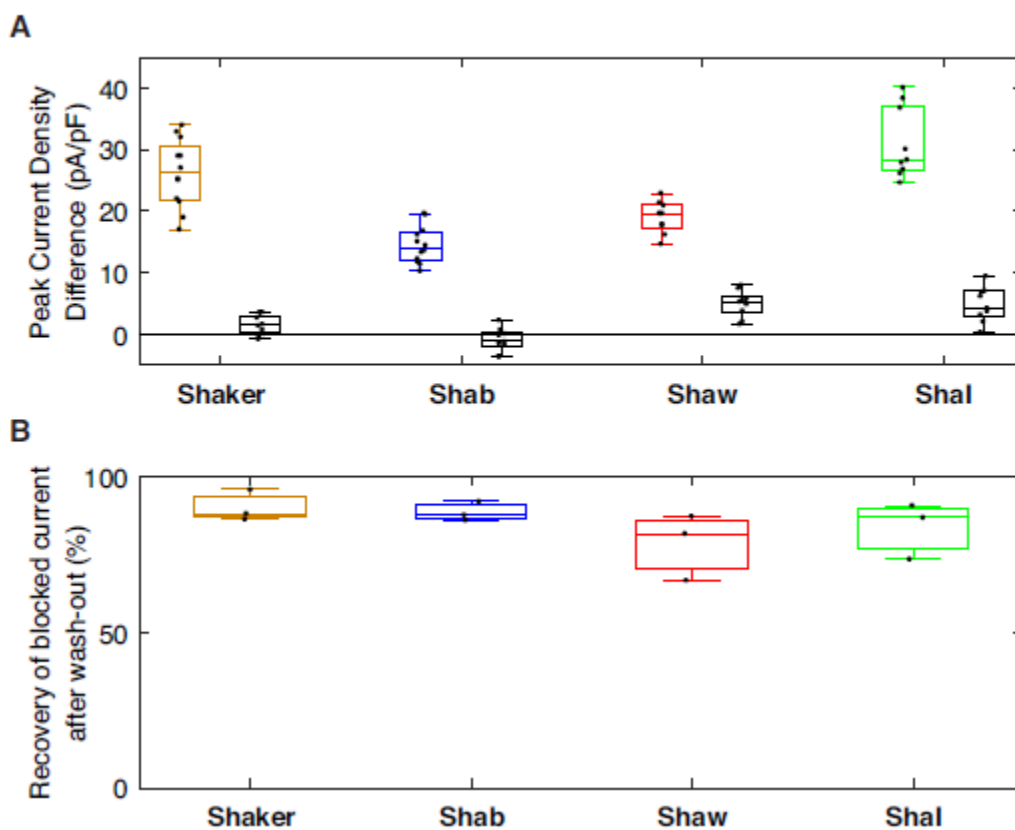

Figure 2

Figure 3: Effects of the molecular clock on membrane clock oscillations in l- and s-LNvs.

A, Peak channel current density at -3 mV at different times of day in LD (grey, lights off; white, lights on) for each of the channels Shaw (left panel, s-LNv: n=12, l-LNv: n=13) and Shal (right panel, s-LNv: n=12, l-LNv: n=12) or **B**, on day 3 of constant darkness (DD) in either small LNvs (s-LNv) or in large LNvs (l-LNv); a similar pattern was seen at other voltages. In LD, Shaw (left panels) and Shal (right panels) rhythms was seen in both s- and l-LNvs. In DD, rhythms persist in Shaw for the s-LNvs (p=0.0229, n=12) but were abolished in the l-LNvs (p=0.7982, n=13). Similarly, rhythms persist in Shal for the s-LNvs (p=0.0006, n=12) but were abolished in the l-LNvs (p=0.4149, n=12). Mean ± SD over three trials per time-point and condition; one-way ANOVA, Tukey's *post-hoc* test. **C,** Peak channel current density in l-LNvs at different times of day in a 12 h:12 h light/dark cycle (LD) (grey, lights off; white, lights on) in control conditions (same as in A), or in LNvs that expressed either CLOCK (CLKΔ5, n=12) or CYCLE DN transgenes (CYCΔ103, n=12). Rhythms were abolished in l-LNvs in the absence of a functional molecular clock even in a standard LD cycle.
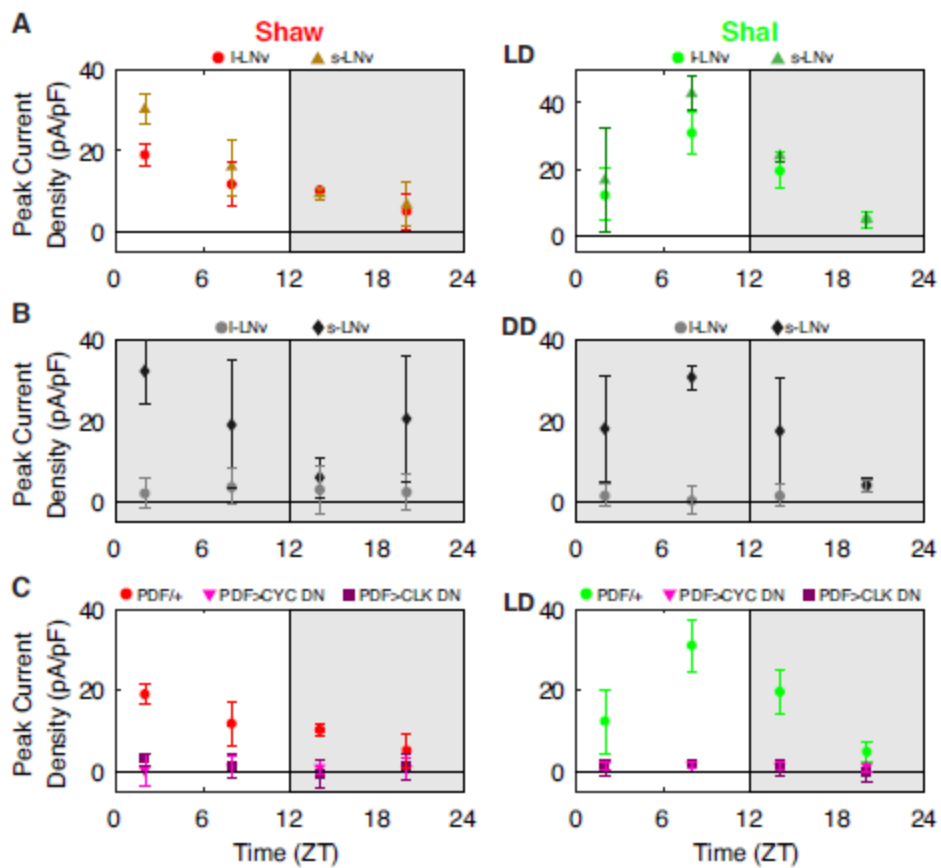
Figure 3

Figure 4: Circadian locomotor activity and longevity effects of reduced Shaw and Shal current.

A, Average activity profiles of flies that expressed Shaw (n=14) and Shal (n=21) DN transgenes in the LNvs compared to control (PDF/+; n=16) over 5 days of LD. Shaded areas represent lights-off and white areas represent lights-on, dots indicate SD. **B,** Rhythmic statistics over days 5-7 of constant darkness (DD). There is no significant effect of DN expression on rhythm strength with either Shaw (p=0.0554) or Shal (p=0.9011) DN expression. Bars represent the mean and error bars represent SD. **C,** Length of rhythm period in DD. There was no significant change with expression of Shal DN (p=0.2518), but there was a small period lengthening with expression of Shaw DN (p<0.0001). **D**, Activity counts of day (left bars) and night (right bars) activity in control flies (PDF/+ n=16, Shaw DN/+ n=15, Shal DN/+ n=20) and flies that expressed the Shaw (Shaw DN, n=14) or Shal (Shal DN, n=21) DN transgenes in the LNvs. In particular, night activity is increased in both Shaw (p<0.0001) and Shal (p<0.0001) DN expression flies compared with undriven controls; similar differences are seen when compared with PDF/+ controls (#). **E,** Longevity of flies. Compared with PDF control flies (median age 75, n=165), expression of either Shaw (median age 64, p<0.0001, n=77) or Shal (median age 61, p<0.0001, n=202) DN significantly reduced lifespan in a Mantel-Cox log-rank test. Undriven Shaw (median age 74, p=0.5166, n=100) and Shal (median age 75, p=0.9805, n=100) controls did not differ from PDF/+ controls.
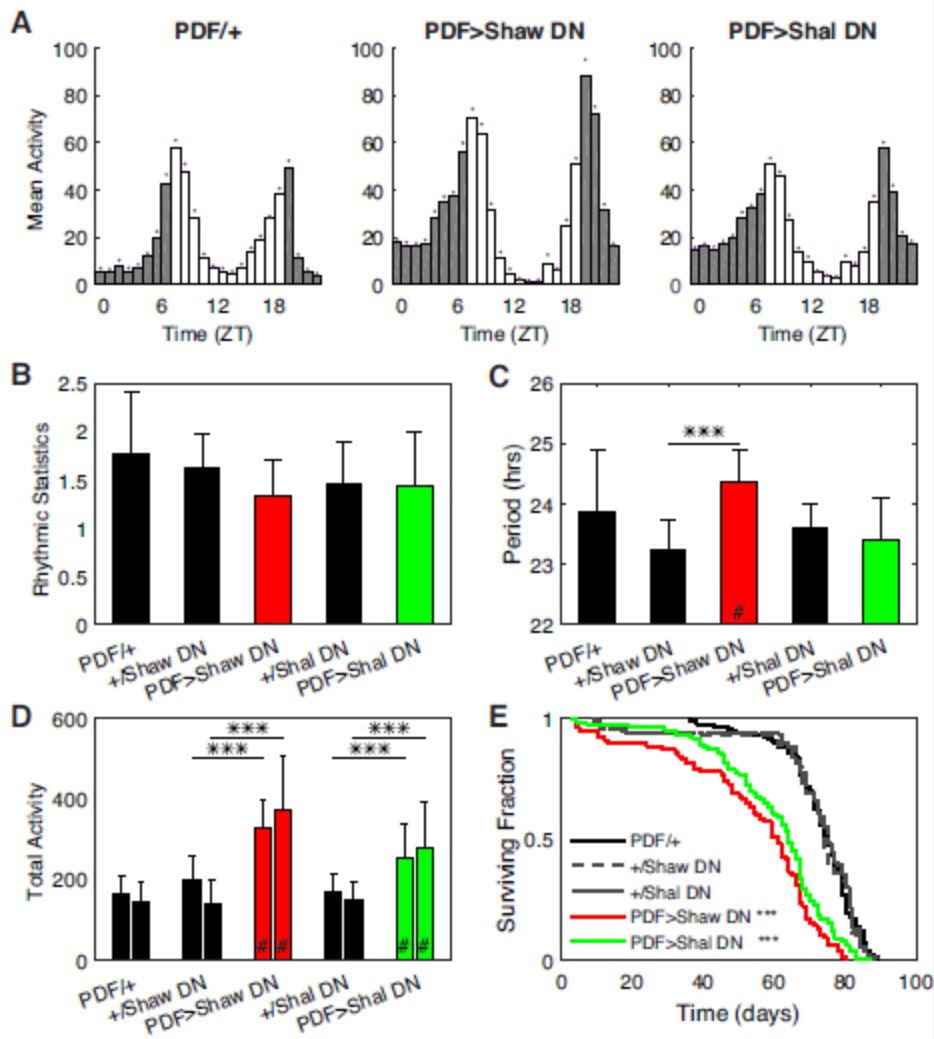
Figure 4

Figure 5: Computational modeling of l-LNv electrophysiological data.

A, 5-second epoch of a representative current-clamp recording of l-LNv electrical activity (upper trace) in the morning (ZT0-2) and the evening (ZT12-14) and a corresponding 5-second epoch of model simulation of electrical activity (lower trace) in the morning and the evening. **B,** Magnification of one action potential in the model simulation (top) in both morning and evening and the underlying voltage-gated potassium channel currents (bottom). The Shaw current was a large contributor to action potential current in the morning, whereas Shal was a large contributor to the action potential in the evening. **C,** Comparison of modelled and recorded action potential firing rate in the morning and evening showed a clear difference for time of day (p<0.001, two-way ANOVA) that was consistent between the model and experimental data. Box and whiskers are median, IQR and min-max, n=20 for each.
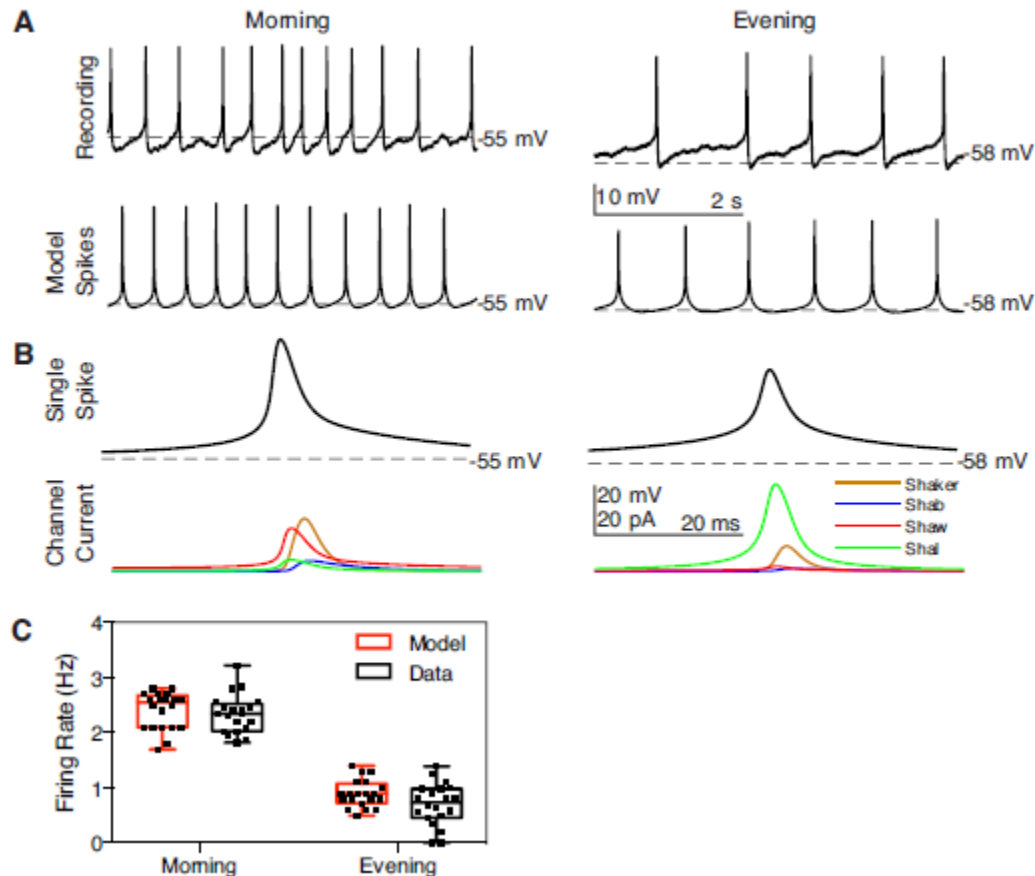

Figure 5

Figure 6: Dynamic clamp models rescue pharmacological block of specific voltage-gated potassium channels.

A, Representative current-clamp recording of l-LNv electrical activity (top row) recorded at ZT6 showing control activity (left panel) application of the Shaker blocker DTX (100 nM) (middle panel) and subsequent reintroduction of Shaker current using dynamic clamp to rescue action potential firing rate (right panel). Dynamic clamp current output during the current-clamp recordings are also shown (bottom row). **B**, Quantification showed the action potential firing frequency before (left) and after (middle) application of the respective channel blockers (DTX n=5, GxTX n=5, BDS n=6, PaTX n=5), and then with the blocker plus the dynamic clamp model (right). Application of all channel blockers can be rescued by use of the dynamic clamp model. Conductances used for dynamic clamp models are given in Table 2.
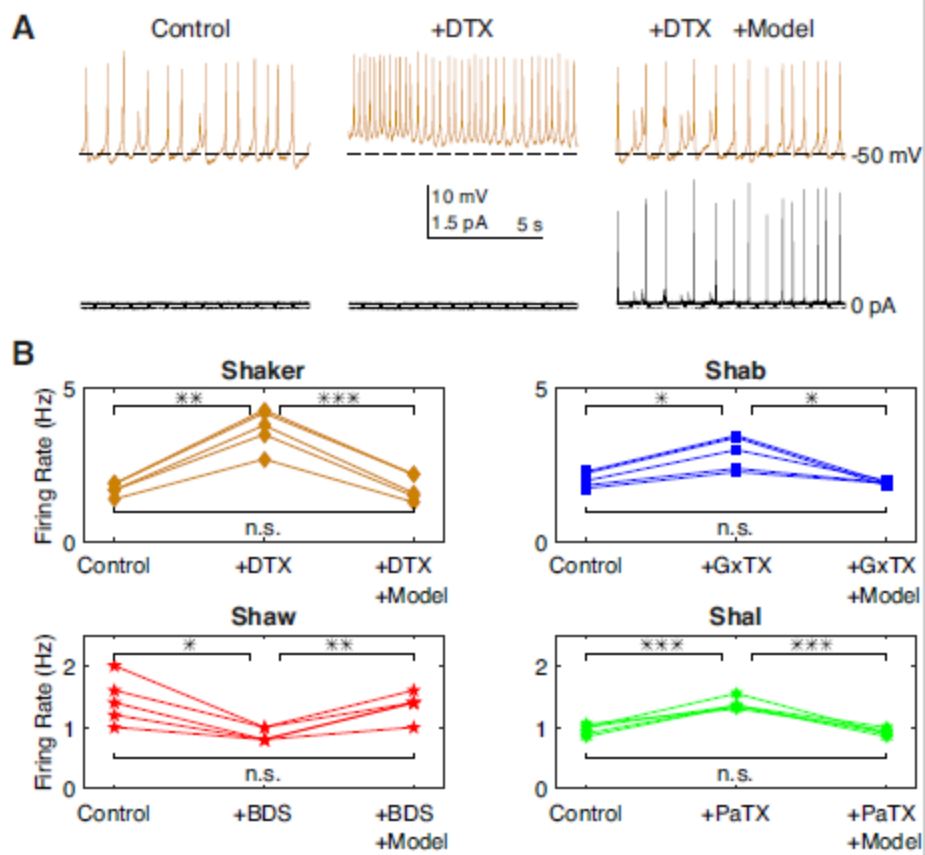
Figure 6

A Control   +DTX   +DTX +Model

10 mV
1.5 pA   5 s

-50 mV

0 pA

B

Shaker

Shab

Shaw

Shal

Figure 7: Switching between morning- and evening-like electrical states of the l-LNvs using dynamic clamp.

A, Representative current-clamp recording (upper trace) and dynamic clamp output (lower trace) of l-LNv electrical activity in the morning showed the characteristic morning action potential firing rate of ~2 Hz. Removal of Shaw current and introduction of Shal current using dynamic clamp switched the firing rate to the evening level of ~1 Hz (left panel). In the evening, introduction of Shaw and removal of Shal switched the firing rate from ~1 Hz to the morning state of ~2 Hz (right panel). **B,** Quantification showed the switch from a morning to an evening state (left panel, p<0.0001, n=4) and from an evening to a morning state (right panel, p<0.0001, n=3). Conductances used for dynamic clamp models are given in Table 3.
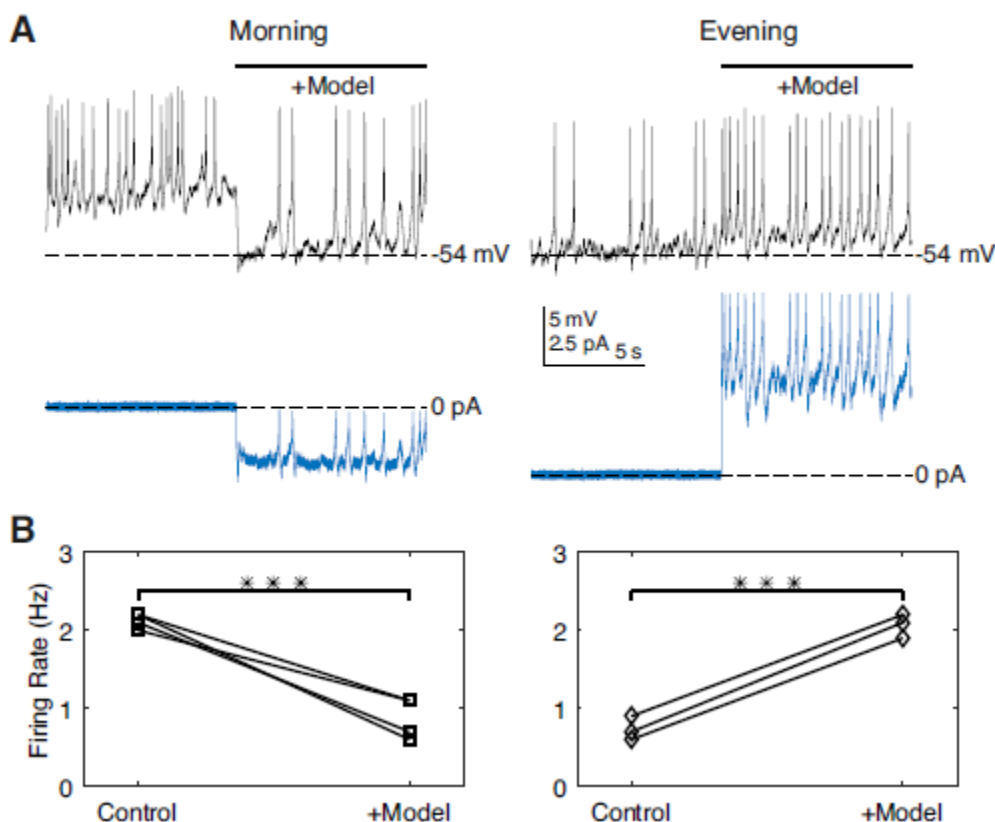
Figure 7

Table 1: **Hodgkin-Huxley equation parameters for ion channel models.** For each of the voltage-gated potassium channel models describing Shaker, Shab, Shaw and Shal, the activation and inactivation parameters and conductances are given as determined by fit to Hodgkin-Huxley equations (see Methods for details).

Activation (m)	Shaker (Kv1)	Shab (Kv2)	Shaw (Kv3)	Shal (Kv4)
Vh (mV)	-34.18	-29.69	-57.30	-48.63
K (mV^{-1})	9.75	10.49	14.63	7.65
Amp (s^{-1})	1.79	30.72	0.03	0.05
Vmax (mV)	-4.07	-63.69	20.03	-74.86
σ (mV^{-1})	73.88	28.54	238.58	61.54
Inactivation (h)				
Vh (mV)	-93.19	NA	-25.82	-43.05
K (mV^{-1})	54.49	NA	2.5	1.73
Amp (s^{-1})	22.49	NA	154.83	44.52
Vmax (mV)	35.81	NA	159.82	-66.24
σ (mV^{-1})	52.04	NA	167.10	180.11
Conductance (nS)	2.35	0.86	1.40	1.25

Table 2: **Dynamic clamp rescue experiment conductances.** For each of the voltage-gated potassium channel models describing Shaker, Shab, Shaw, and Shal, the conductances used to rescue pharmacological block of the channel are given (see Figure 6).

Conductance (nS)	Shaker (Kv1)	Shab (Kv2)	Shaw (Kv3)	Shal (Kv4)
	2.35	0.86	1.40	0.8
	2.05	0.66	1.40	0.8
	1.90	0.66	1.30	0.8
	1.60	0.44	1.30	0.8

Table 3: **Dynamic clamp day/night switching experiment conductances.** For the voltage-gated potassium channel models describing Shaw and Shal, the conductances used to switch the l-LNvs between morning and evening firing states are given (see Figure 7).

Conductance (nS)	Shaw (Kv3)	Shal (Kv4)
Day to Night	-1.4	1.25
	-1.2	1.15
	-1.1	1.00
	-0.8	0.90

First author profile
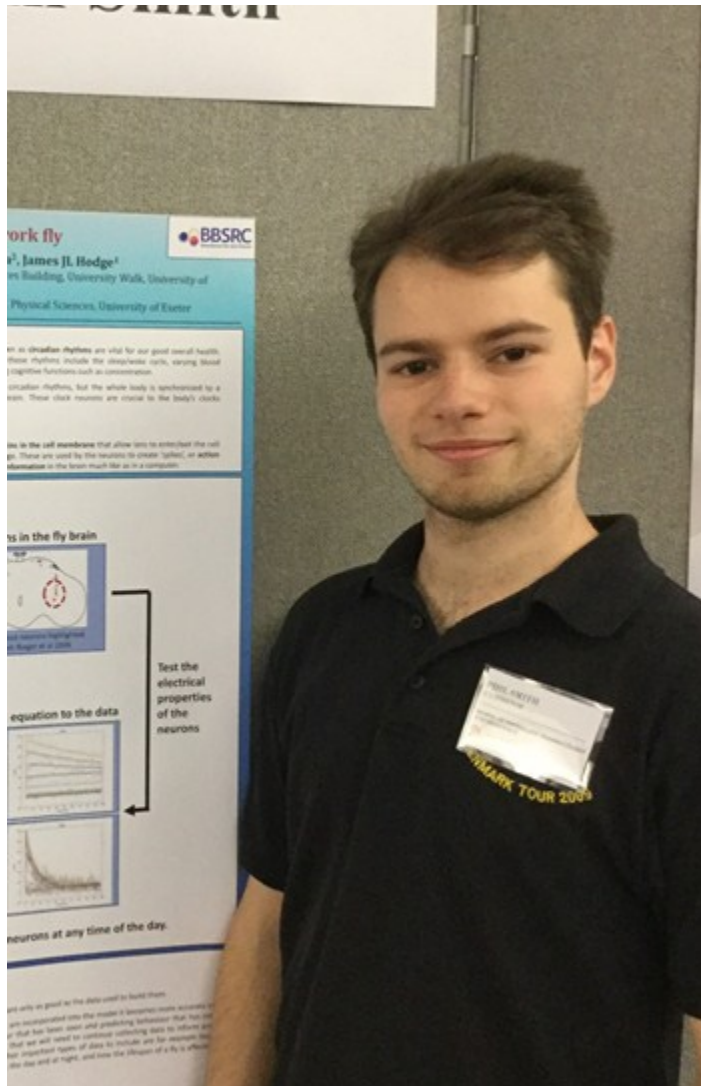
Dr Philip Smith graduated with a PhD from the School of Physiology, Pharmacology and Neuroscience, at the University of Bristol in 2019. He studied in the lab of Professor James Hodge the role of voltage-gated potassium channels in *Drosophila* using electrophysiology, pharmacology, genetics and behaviour. He also learned mathematical and computational modelling with Professor Krasimira Tsaneva-Atanasova at the University of Exeter. As a team they have published the first *Drosophila* model of essential tremor based on Kv9 channel mutations and previously published on P2X7 electrophysiology. Phil is now working in technology transfer in Cancer Research UK and the NHS.